Postprint of: Pietrenko-Dabrowska, A. and Koziel, S., Expedited antenna optimization with numerical derivatives and gradient change tracking, Engineering Computations, Vol. 37 No. 4 (2019), pp. 1179-1193 DOI: 10.1108/EC-04-2019-0155

Expedited Antenna Optimization with Numerical Derivatives and Gradient Change Tracking

Anna Pietrenko-Dabrowska[1] and Slawomir Koziel[1,2]

[1] Faculty of Electronics, Telecommunications and Informatics, Gdansk University of Technology, 80-233 Gdansk, Poland, anna.dabrowska@pg.edu.pl

[2] Engineering Optimization & Modeling Center, Reykjavik University, 101 Reykjavik, Iceland, koziel@ru.is

Expedited Antenna Optimization with Numerical Derivatives and Gradient Change Tracking

Keywords: Antenna design, input characteristics, computer-aided design, simulation-driven design, trust-region methods, updating formulas.

Structured Abstract

Purpose

A framework for expedited antenna optimization with numerical derivatives involving gradient variation monitoring throughout the optimization run is proposed and demonstrated using a benchmark set of real-world wideband antennas. A comprehensive analysis of the algorithm performance involving multiple starting points is provided. The optimization results are compared with a conventional trust-region procedure, as well as the state-of-the-art accelerated trust-region algorithms.

Design/methodology/approach

The proposed algorithm is a modification of the trust-region gradient-based algorithm with numerical derivatives, in which a monitoring of changes of the system response gradients is performed throughout the algorithm run. The gradient variations between consecutive iterations are quantified by an appropriately developed metric. Upon detecting stable patterns for particular parameter sensitivities, the costly finite-differentiation-based gradient updates are suppressed, hence the overall number of full-

wave electromagnetic simulations is significantly reduced. This leads to considerable computational savings without compromising the design quality.

Findings

Monitoring of the antenna response sensitivity variations during the optimization process enables us to detect the parameters for which updating the gradient information is not necessary at every iteration. When incorporated into the trust-region gradient-search procedures, the approach permits reduction of the computational cost of the optimization process. The proposed technique is dedicated to expedite direct optimization of antenna structures, but it can also be applied to speed up surrogate-assisted tasks, especially solving sub-problems that involve performing numerous evaluations of coarse-discretization models.

Research limitations/implications

The introduced methodology opens up new possibilities for future developments of accelerated antenna optimization procedures. In particular, the presented routine can be combined with the previously reported techniques that involve (i) replacing finite differentiation with the Broyden formula for directions that are satisfactorily well aligned with the most recent design relocation and/or (ii) performing finite differentiation in a sparse manner based on relative design relocation (with respect to the current search region) in consecutive algorithm iterations.

Originality/value

Benchmarking against a conventional trust-region procedure, as well as previously reported methods confirm improved efficiency and reliability of the proposed approach.

The applications of the framework include direct EM-driven design closure, along with surrogate-based optimization within variable-fidelity surrogate-assisted procedures. To our knowledge, no comparable approach to antenna optimization has been reported elsewhere. Particularly, it surmounts established methodology by carrying out constant supervision of the antenna response gradient throughout successive algorithm iterations and utilizing gathered observations to properly guide the optimization routine.

Abstract

Design automation has been playing an increasing role in the development of novel antenna structures for various applications. One of its aspects is electromagnetic (EM)-driven design closure, typically applied upon establishing the antenna topology, and aiming at adjustment of geometry parameters to boost the performance figures as much as possible. Parametric optimization is often realized using local methods given usually reasonable quality of the initial designs obtained at the topology evolution stage. The major difficulty here is high computational cost associated with a large number of EM simulations required by conventional methods, both gradient and derivative-free routines. Possible workarounds including surrogate-assisted variable-fidelity methods (e.g., space mapping) face similar problems because the underlying low-fidelity model is often optimized directly. This paper proposes an expedited version of the trust-region (TR) gradient-based algorithm with numerical derivatives. A considerable reduction of the number of EM simulations is achieved by monitoring the behavior of the gradient throughout the algorithm run and omitting the finite-differentiation updates upon detecting stable patterns for particular parameter sensitivities. The proposed approach is benchmarked against the standard TR algorithm as well as the recently reported accelerated TR frameworks. Improved performance is consistently demonstrated for all considered test cases.

1. Introduction

Design of modern antennas is a comprehensive process that consists of several stages, involving conceptual development, topology evolution interleaved with parametric studies (Saini and Dwari, 2016; Vendik *et al.*, 2017), and typically concluded by a tuning of geometry parameter values (Ullah and Koziel, 2018; Lalbakhsh *et al.*, 2019). The importance of this last step has been increasing over the years for several reasons. These include a growing complexity of antenna designs, a large number of variables necessary to parameterize antenna geometries, but also the need to handle multiple performance figures and constraints (Koziel and Bekasiewicz, 2016; Lalbakhsh *et al.*, 2017a). Thereupon, traditional methods predominantly based on supervised parameter sweeping, become inadequate. Appropriate control over multi-dimensional parameter spaces, objectives and constraints requires rigorous numerical optimization. However, apart from some trivial setups (e.g., antenna array pattern synthesis involving analytical array models that ignore mutual coupling effects (Goudos *et al.*, 2011; Reyna *et al.*, 2017)), design closure has to be carried out at the level of electromagnetic (EM) simulation models. This induces practical problems, primarily related to the high cost of massive EM simulations required by conventional optimization algorithms (Nocedal and Wright, 2006). The issue is especially pronounced when global optimization is necessary, typically executed using tremendously expensive population-based metaheuristics (Choi *et al.*, 2016; Zaharis *et al.*, 2017).

A practical necessity led to the development of various methods for mitigating the problem of excessive costs of EM-driven design closure. The following two (although partially overlapping) groups of approaches can be distinguished: algorithmic

improvements and utilization of (global) replacement models. The first class includes gradient-based procedures with adjoint sensitivities (Ghassemi *et al.*, 2013; Wang *et al.*, 2018)—very efficient but not widespread due to limited availability of adjoints through commercial EM solvers)—as well as surrogate-assisted frameworks (e.g., response correction techniques (Koziel and Ogurtsov, 2014), space mapping (Baratta *et al.*, 2018), manifold mapping (Su *et al.*, 2017), adaptive response scaling (Koziel and Unnsteinsson, 2018), feature-based optimization (Koziel, 2015)). Utilization of these techniques for antenna design is hindered by the lack of fast underlying low-fidelity models. Within the second group, the most popular approaches are those involving data-driven (or approximation) surrogates such as kriging (de Villiers *et al.*, 2017) or Gaussian process regression (Jacobs, 2016), also combined with machine learning methods (Liu *et al.*, 2016), as well as artificial neural networks (Chavez-Hurtado and Rayas-Sanchez, 2016) or support-vector regression (Cai *et al.*, 2018). Unfortunately, due to the curse of dimensionality, utilization of data-driven models is limited to antenna topologies described by a few parameters (de Villiers *et al.*, 2017) or local applications (e.g., statistical analysis (Koziel and Bekasiewicz, 2018). Data-driven models are also employed in the design of other high-frequency devices, such as bandpass frequency selective surfaces (Lalbakhsh *et al.*, 2015) or artificial electromagnetic conductor (Lalbakhsh *et al.*, 2017b).

In most practical cases, local optimization routines are applied because the initial designs obtained in the course of antenna topology evolution and parametric studies are reasonably good. This is pertinent to both direct optimization of the high-fidelity EM models and variable-fidelity surrogate-assisted frameworks where the EM-based surrogate model is optimized directly at certain stages of the process. A technique for expediting

trust-region (TR) gradient search has been proposed in Koziel and Pietrenko-Dabrowska, 2019a, where the main mechanism involved sparse gradient updates controlled by design relocation between algorithm iterations. Considerable computational savings were demonstrated, yet obtained at the expense of design quality degradation. A different approach proposed in Koziel and Pietrenko-Dabrowska, 2019b yields an even better efficiency but without fixing the quality issue. In this paper, an alternative TR-based technique is proposed where a reduction of the number of EM simulations is achieved by monitoring the changes and variability of the antenna response sensitivities across the algorithm iterations. Stability of particular gradient components is quantified by appropriately developed metrics and promotes gradient updates suppression involving finite-differentiation (FD). As demonstrated using several antenna examples, the proposed approach ensured better efficiency than in Koziel and Pietrenko-Dabrowska, 2019a and Koziel and Pietrenko-Dabrowska, 2019b (average speedup of up to 45 percent as compared to the reference algorithm) but without compromising the design quality.

2. Expedited Gradient Search by Means of Gradient Change Monitoring

This section recalls the formulation of a design closure task, outlines the trust-region gradient search algorithm (a popular solution approach for EM-driven design problems), as well as introduces the proposed expedited version of the procedure.

2.1. EM-Driven Design Closure. Problem Formulation

Contemporary antennas must fulfill specifications imposed on various electrical and field characteristics of the device. Design closure involves final tuning of geometry parameters and improve its performance as much as possible. For that, a quality measure

is necessary and in majority of practical implementations of EM-based tuning it is a scalar function of the parameters (genuine multi-objective design, Koziel and Bekasiewicz, 2016, is out of the scope of this paper). In the presence of multiple objectives, a primary one can be selected with the remaining ones controlled through appropriately defined constraints. Using this approach, the design closure task may be defined as ($\boldsymbol{x}$ being a vector of geometry parameters)

$$\boldsymbol{x}^* = \arg\min_{\boldsymbol{x}} U(\boldsymbol{x}) \tag{1}$$

subject to $g_k(\boldsymbol{x}) \leq 0$, $k = 1, \ldots, n_g$, and $h_k(\boldsymbol{x}) = 0$, $k = 1, \ldots, n_h$ (inequality and equality constraints, respectively). As most of the constraints are computationally expensive (require EM simulation), a penalty function approach is a convenient way of handling these (Conn *et al.*, 2000). The problem is then reformulated as

$$\boldsymbol{x}^* = \arg\min_{\boldsymbol{x}} U_P(\boldsymbol{x}) \tag{2}$$

with

$$U_P(\boldsymbol{x}) = U(\boldsymbol{x}) + \sum_{k=1}^{n_g+n_h} \beta_k c_k(\boldsymbol{x}) \tag{3}$$

where $c_k(\boldsymbol{x})$ measure violations of the respective constraints whereas β_k are the penalty coefficients. A few examples follow:

1. Best matching design: $U(\boldsymbol{x}) = S(\boldsymbol{x}) = \max\{f \in F : |S_{11}(\boldsymbol{x},f)|\}$, where f is a frequency within a range of interest F.
2. Gain maximization: $U(\boldsymbol{x}) = -G(\boldsymbol{x})$, where $G(\boldsymbol{x})$ is the average in-band gain, with the constraint $S(\boldsymbol{x}) \leq -10$ dB.
3. Axial ratio improvement: $U(\boldsymbol{x}) = AR(\boldsymbol{x})$, where $AR(\boldsymbol{x})$ is the maximum in-band axial ratio; constraint $S(\boldsymbol{x}) \leq -10$ dB.

4. Size reduction of a CP antenna: $U(\boldsymbol{x}) = A(\boldsymbol{x})$, where $A(\boldsymbol{x})$ is the footprint; constraints $S(\boldsymbol{x}) \leq -10$ dB and $AR(\boldsymbol{x}) \leq 3$ dB.

A typical form of the penalty function would be relative constraint violation, e.g., $c(\boldsymbol{x}) = [(S(\boldsymbol{x}) + 10)/10]^2$ for S_{11} (second power used to ensure the smoothness of U_P at the feasible region boundary). The above examples do not constitute an exhaustive list. Another possible application is pattern synthesis (e.g., side lobe level reduction), especially when full-wave EM models are used to antenna array evaluation (e.g., in order to take into account mutual coupling effects), in which case local optimization methods would normally be applied due to excessive costs of global routines (Bencivenni *et al.*, 2016; Siragusa *et al.*, 2012). This is especially the case when handling very large arrays, in particular reflectarrays, comprising up to thousands of elements (Zhou *et al.*, 2015; Richard *et al.*, 2019; Prado *et al.*, 2019).

2.2. Trust-Region-Embedded Gradient Search

The trust-region (TR) gradient-based algorithm (e.g., Conn *et al.*, 2000) is used here as the reference method. It solves the problem (2) by generating vectors $\boldsymbol{x}^{(i)}$, $i = 0, 1, \ldots$, as approximations to $\boldsymbol{x}^*$, obtained through optimization of a linear expansion model $U_L^{(i)}$ of U_P at $\boldsymbol{x}^{(i)}$. The model $U_L^{(i)}$ is defined similarly as U_P but using expansion models of the respective antenna responses. For example, for the reflection characteristic, we have

$$S_L^{(i)}(\boldsymbol{x}, f) = S_{11}(\boldsymbol{x}^{(i)}, f) + \boldsymbol{G}_S(\boldsymbol{x}^{(i)}) \cdot (\boldsymbol{x} - \boldsymbol{x}^{(i)}) \tag{4}$$

and so on, where $\boldsymbol{G}_S$ stands for the reflection gradient. The approximation vectors are found as

$$\boldsymbol{x}^{(i+1)} = \arg \min_{\boldsymbol{x};\, -\boldsymbol{d}^{(i)} \leq \boldsymbol{x} - \boldsymbol{x}^{(i)} \leq \boldsymbol{d}^{(i)}} U_L^{(i)}(\boldsymbol{x}) \tag{5}$$

For the later use, we denote sensitivity matrix corresponding to all antenna responses collectively as $\boldsymbol{G}$, and it is estimated using finite differentiation; $\boldsymbol{d}^{(i)}$ is the search region size

vector adjusted using the standard rules (Conn *et al.*, 2000). The inequalities $-\boldsymbol{d}^{(i)} \le \boldsymbol{x} - \boldsymbol{x}^{(i)} \le \boldsymbol{d}^{(i)}$ in (5) are component-wise. Interval-type definition of the trust region eliminates the need for variable scaling by making the initial size vector $\boldsymbol{d}^{(0)}$ proportional to the design space sizes. The CPU cost of each algorithm iteration is at least $n + 1$ EM antenna simulations necessary to evaluate the system response and the gradient. For unsuccessful iterations, the cost increases because the candidate design has to be reset by solving (5) with a reduced $\boldsymbol{d}^{(i)}$ and re-evaluated.

2.3. Gradient Change Monitoring for TR Framework Acceleration

In the proposed technique, the behavior of the gradient of the antenna characteristics throughout the algorithm run is monitored, in order to pinpoint the parameters characterized by stable sensitivity patterns. For such parameters, the finite-differentiation-based update may be skipped. The gradient changes are quantified by a metric introduced below; if they are minor, the FD estimation is not performed.

For the sake of explanations, let us assume that the antenna characteristic of interest is the reflection coefficient $S_{11}(\boldsymbol{x},f)$, here, being a function of the antenna designable parameter vector $\boldsymbol{x}$ and the frequency f. Let us denote as $\boldsymbol{G}_S = [G_1 \ \ldots \ G_n]^T$ the gradient vector of $S_{11}(\boldsymbol{x},f)$, where G_k denotes sensitivity w.r.t the k-th parameter, $k = 1, \ldots, n$. In addition, let $G_k^{(i)}(f)$ and $G_k^{(i-1)}(f)$ refer to the k-th component of the gradient $\boldsymbol{G}_S$ in the ith and $(i-1)$th iteration, respectively (the gradient dependence on the frequency f is shown explicitly). In order to compare $G_k^{(i)}$ and $G_k^{(i-1)}$ at two subsequent iterations, the gradient change factors (averaged over the frequency range of interest F) are utilized as a quantification metric

$$d_k^{(i+1)} = \underset{f \in F}{mean}\left(2 \cdot \frac{\left|G_k^{(i)}(f)\right| - \left|G_k^{(i-1)}(f)\right|}{\left|G_k^{(i)}(f)\right| + \left|G_k^{(i-1)}(f)\right|} \right) \tag{6}$$

In the i-th iteration, the minimum and the maximum value of gradient change factors of all parameters: $d_{\min}^{(i)} = \min\{k = 1, \ldots, n : d_k^{(i)}\}$ and $d_{\max}^{(i)} = \max\{k = 1, \ldots, n : d_k^{(i)}\}$, respectively, is found. Using these, a number $N_k^{(i)}$ of future iterations without FD for the k-th parameter is assessed. The relationship between $N_k^{(i)}$ and the factors $d_k^{(i)}$ is described by the affine conversion function

$$N_k^{(i)} = \text{⟦} \qquad \text{⟧} \tag{7}$$

where $a^{(i)} = (N_{\max} - N_{\min})/(d_{\min}^{(i)} - d_{\max}^{(i)})$ and [[.]] denotes the nearest integer function. In addition, $N_{\min}$ and $N_{\max}$ refer to the minimum and the maximum number of iterations without FD (the algorithm control parameters). Clearly, the maximum number $N_{\max}$ is assigned to the parameters featuring the smallest gradient change between subsequent iterations, as quantified by $d_k^{(i)}$. An increase in $d_k^{(i)}$ leads to a decrease of $N_k^{(i)}$. The sensitivity update through FD is carried out at least once per $N_{\max}$ iterations, and not more often than every $N_{\min}$ iterations. The value of $N_k^{(i)}$ is based both on the "current" difference factors $d_k^{(i)}$ (calculated using (6) for the parameters with FD performed in the i-th iteration), as well as the "prior" ones (retained from the previous iterations for the parameters without FD in the i-th iteration).

Figure 1 shows the operation of the proposed algorithm in a form of a flow diagram. In each iteration, a binary selection vector $\boldsymbol{\alpha}^{(i)}$ is created. The nonzero entries $\alpha_k^{(i)}$, $k = 1, \ldots, n$, refer to the variables for which the gradient component $G_k^{(i)}$ is to be updated using FD. Conversely, $\alpha_k^{(i)}$ equal to zero implies omission of FD. In the first two iterations, the entire gradient is estimated solely using FD. From the third iteration on (see Fig. 1), the

components of the selection vector $\alpha_k^{(i)}$ are derived from the $N_k^{(i)}$ as follows: $\alpha_k^{(i)} = 1$ if $N_k^{(i)} = 1$, and $\alpha_k^{(i)} = 0$ if $N_k^{(i)} > 1$. The values $N_k^{(i+1)}$ for the $(i+1)$th iteration are determined using (7) for the variables currently updated through FD, whereas for the remaining parameters the previously assigned number of iterations is decremented, i.e., $N_k^{(i+1)} = N_k^{(i)} - 1$. Consequently, in each iteration, the gradient $\boldsymbol{G}_S$ is merged from the entries either currently estimated with FD (if $\alpha_k^{(i)} = 1$) or previously estimated with FD (if $\alpha_k^{(i)} = 0$).

The proposed algorithm with the gradient change tracking follows the operation of the reference algorithm of Section 2.2 merely in the first two iterations. The major difference is a conscientious omission of FD updates in subsequent iterations governed by the gradient stability pattern. The numerical results summarized in Section 3 indicate that the proposed procedure delivers considerable CPU cost savings, at the expense of a slight deterioration of the design quality.

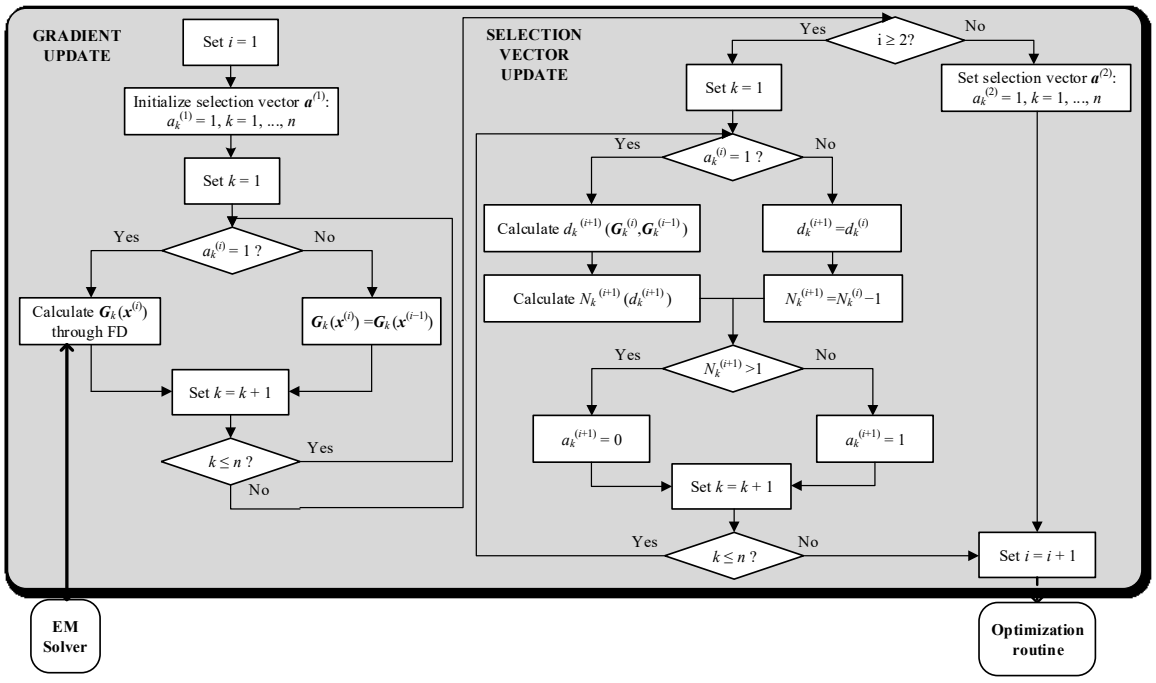

Fig. 1. Flow diagram the proposed algorithm with gradient change control.

3. Verification Case Studies

Our benchmark set comprises three wideband antenna structures. Antenna I (Qing and Chen, 2009), shown in Fig. 2(a), is a uniplanar structure with a driven element in the form of a fork-shaped radiator fed through a coplanar waveguide. It is implemented on Taconic RF-35 substrate (h = 0.762 mm, ε_r = 3.5, tanδ = 0.0018) and its independent geometry variable vector is $\boldsymbol{x} = [l_0\ l_1\ l_{2r}\ l_{3r}\ l_4\ l_5\ w_1\ w_2\ w_3\ w_4\ g]^T$, with $l_2 = (0.5w_f + s + w_1)\cdot\max\{l_{2r}, l_{3r}\}$ and $l_3 = (0.5w_f + s + w_1)\cdot l_{3r}$; w_f = 3.5 and s = 0.16 fixed to ensure 50 ohm input impedance. Antenna II, (Fig. 2(b)), is also implemented on the same substrate and it comprises a quasi-circular radiator and a modified ground plane for bandwidth enhancement (Alsath and Kanagasabai, 2015). The design variables are: $\boldsymbol{x} = [L_0\ dR\ R\ r_{rel}\ dL\ dw\ L_g\ L_1\ R_1\ dr\ c_{rel}]^T$. Antenna III (Haq *et al.*, 2017), shown in Fig. 2(c), is implemented on FR4 substrate (ε_r = 4.3, and h = 1.55 mm) and its geometry parameters are $\boldsymbol{x} = [L_g\ L_0\ L_s\ W_s\ d\ dL\ d_s\ dW_s\ dW\ a\ b]^T$. The computational models for all antennas are implemented in CST Microwave Studio and evaluated using its transient solver. All models incorporate SMA connectors. The model setups are the following: Antenna I: ~550,000 mesh cells, simulation time 130 seconds; Antenna II: ~830,000 mesh cells, simulation time 210 seconds; and Antenna III: ~520,000 mesh cells, simulation time 176 seconds.

The antennas have been optimized for minimum reflection within the UWB band (3.1 GHz to 10.6 GHz) as formulated in Section 2. The proposed algorithm has been executed with $N_{\min}$ = 1 and $N_{\max}$ = 5 and 7. In order to properly assess the performance of the optimization routine, ten random initial designs have been used for each antenna. The reason for executing multiple runs of the algorithm is that all of the considered optimization problems are, as a matter of fact, multimodal. This primarily results from the parametric

redundancy, which, in turn, comes from various topological modifications introduced within the antenna geometries (all of the cases are compact antennas that contain modifications aimed at footprint area reduction). Consequently, starting from different initial designs, the local routine ends up in somehow different local optima. These optima are all of satisfactory quality yet distinct. Benchmarking made on the basis of multiple runs gives a more representative picture of the algorithm performance because of reducing the bias associated with selecting a particular initial design.

The result statistics are presented in Table I. For comparison, Antennas I through III have been optimized using the reference algorithm of Section 2.2 (Algorithm 1). The comparison with previously reported algorithms is also given: Algorithm 2 (Koziel and Pietrenko-Dabrowska, 2019a) and Algorithm 3 (Koziel and Pietrenko-Dabrowska, 2019b; for the basic theory see Appendix). The results for the presented algorithm with $N_{\max} = 5$ and 7 are given in Table I as well (Algorithm 4 and 5, respectively). Table II provides a thorough comparison of the main features of the aforementioned algorithms. The plots of the initial and optimized responses for the representative algorithm runs for all benchmark antennas are presented in Fig. 3.

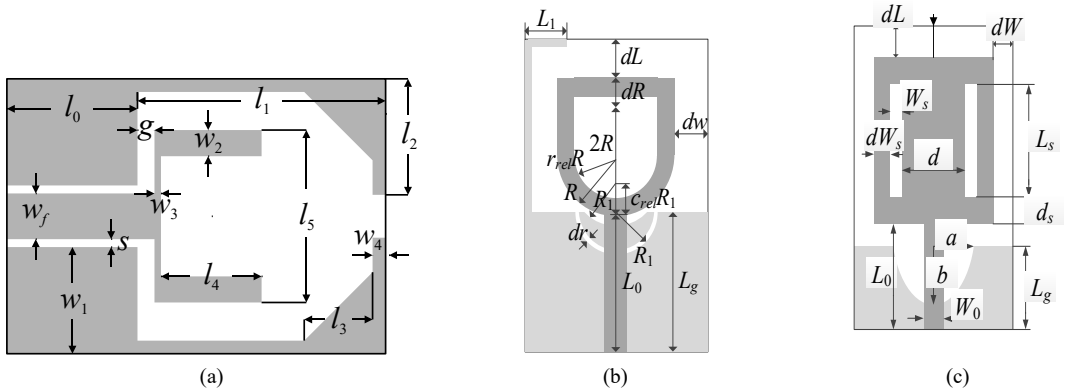

Fig. 2. Benchmark antenna structures used for verification of the proposed algorithm: (a) Antenna I, (b) Antenna II, (c) Antenna III. The ground plane marked using light gray shade.

Table I. Optimization Results for Antennas I through III, along with Computational Savings, Design Quality Degradation and Results Repeatability

	Antenna I					Antenna II					Antenna III				
Algorithm	Cost[a]	Cost savings[b] [%]	max|S_{11}|[c]	Δmax |S_{11}|[d] [dB]	std max|S_{11}|)[e]	Cost[a]	Cost savings[b] [%]	max|S_{11}|[c]	Δmax |S_{11}|[d] [dB]	std max|S_{11}|)[e]	Cost[a]	Cost savings[b] [%]	max|S_{11}|[c]	Δmax |S_{11}|[d] [dB]	std max|S_{11}|)[e]
1	96.5 [209.1]	–	–21.7 [–21.0]	–	0.9	111.2 [389.2]	–	−14.9 [–14.2]	–	0.6	111.0 [325.6]	–	−13.9 [–12.4]	–	1.0
2	70.9 [153.6]	26.5	–20.9	0.8	2.3	58.3 [204.1]	47.6	–13.7	1.2	1.3	73.1 [214.4]	34.1	–12.8	1.1	1.3
3	63.3 [137.2]	34.4	–20.8	0.9	3.4	75.9 [265.7]	31.7	–14.3	0.9	1.0	80.0 [234.7]	27.9	–11.9	1.9	2.0
4	55.6 [120.5]	42.4	–21.9	–0.2	1.0	66.3 [232.1]	40.4	–14.7	0.2	0.8	68.7 [201.5]	38.1	–13.5	0.4	1.1
5	55.5 [120.3]	42.5	–21.8	–0.1	1.0	61.2 [214.2]	45.0	–14.5	0.4	0.9	57.6 [169.0]	48.1	–13.1	0.8	1.2

[a] Number of EM simulations averaged over 10 algorithm runs. The values in brackets below stand for optimization time [min] obtained with Intel Xeon 2.1 GHz dual-core CPU, 128 GB RAM.
[b] Relative computational savings in percent w.r.t. the reference algorithm.
[c] Maximum in-band reflection max|S_{11}| in dB averaged over 10 algorithm runs. The values in brackets below are obtained by the reference algorithm within the overall optimization time of Algorithm 5.
[d] Degradation of max|S_{11}| w.r.t. the reference algorithm in dB.
[e] Standard deviation of max|S_{11}| in dB across the set of 10 algorithm runs.
[1] Reference TR region algorithm (gradient updated solely using FD).
[2] Algorithm of Koziel and Pietrenko-Dabrowska, 2019a (smart gradient update scheme based on relative design relocation during optimization run).
[3] Algorithm of Koziel and Pietrenko-Dabrowska, 2019b (sparse update scheme using Broyden formula based on the alignment of the most recent design relocation with coordinate system axes).
[4, 5] This work, gradient change control algorithm: N_{max} = 5 and 7, respectively.

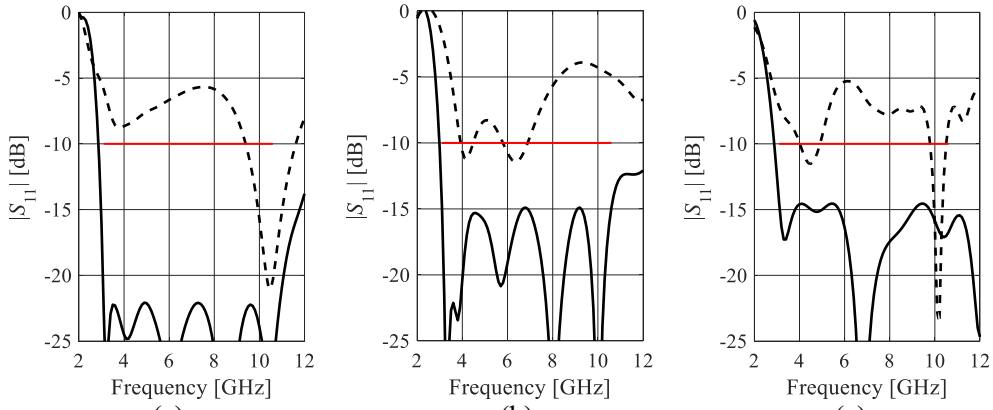

Fig. 3. Reflection responses of the considered antennas for the representative algorithm runs: (a) Antenna I, (b) Antenna II, (c) Antenna III. Horizontal lines mark the design specifications; (- - -) initial design, (—) optimized design.

Table II. Main Features of the Optimization Procedures Utilized in this Work (Including Benchmarking)

	Algorithm	Initial gradient estimation	Acceleration rationale	Finite differentiation gradient update	Average quality deterioration w.r.t. Algorithm 1	Average cost savings w.r.t. Algorithm 1
1	Reference trust-region	finite differentiation	N/A	Performed in each iteration for each parameter	N/A	N/A
2	Algorithm of Koziel and Pietrenko-Dabrowska, 2019a	finite differentiation	relative design relocation w.r.t. trust region size	Omitted in some iterations for some parameters	~1 dB	~35 %
3	Algorithm of Koziel and Pietrenko-Dabrowska, 2019b	finite differentiation	alignment of the design relocation with coordinate system axes	Replaced in some iterations for some parameters with Broyden formula	> 1 dB	~30 %
4	Algorithm of Section 2.3 (N_{max} = 5)	finite differentiation	measure of changes of the response gradient between iterations	Omitted in some iterations for some parameters	~0.2 dB	~40 %
5	Algorithm of Section 2.3 (N_{max} = 7)	finite differentiation	measure of changes of the response gradient between iterations	Omitted in some iterations for some parameters	~0.5 dB	~45 %

The results confirm that the proposed algorithm performs consistently over the considered benchmark set and delivers designs of fine quality (cf. Table I and Fig. 3). It should be underlined, that the solution quality obtained for Antenna I with Algorithm 4 (N_{max} = 5) is even better than that of the reference algorithm. For Antennas II and III, Algorithm 4 delivers designs of insignificantly deteriorated quality: a degradation w.r.t. the reference algorithm is only 0.2 dB and 0.4 dB, respectively. In addition, a considerable computational speedup of 40 percent on average is obtained (from around 38 percent, for Antenna I, to 45 percent for Antennas II and III). The results repeatability is measured by the standard deviation of the objective function value over the set of ten algorithm runs. The results of Table I verifies the reliability of the proposed algorithm, since the obtained values of the standard deviation are only slightly higher than those for the reference algorithm.

In Table I, the results obtained using the two values of algorithm control parameter are presented: N_{max} = 5 and 7. Clearly, increasing N_{max} (Algorithm 5), i.e., omitting FD for a greater number of iterations, further accelerates the optimization process. The average cost savings rise up to 45 percent, which is, however, accompanied by a more pronounced degradation of the solution quality (up to 0.8 dB for Antenna III). The higher value of N_{max}, however, does not influence standard deviation.

It should be noted that because the only objective of the optimization process was matching improvement, there was no control over other performance figures such as the radiation pattern or the physical dimensions of the antenna. As the improvement of the antenna matching (especially at the lower end of the operating frequency range) and the reduction of the footprint area are partially conflicting objectives, it is expected that the optimized designs would exhibit increased size. This is indeed the case. For the specific cases shown in Fig. 3, the footprints before and after optimization are as follows: 716 mm^2, 550 mm^2, 509 mm^2 (Antenna I, II, and III, at the initial design), and 746 mm^2, 575 mm^2, 468 mm^2 (Antenna I, II, and III, optimized), which generally confirms the above prediction (however, note that Antenna III has it footprint reduced upon optimization). On the other hand, the radiation patterns are expected to be relatively stable under the optimization because the antenna topologies are fixed. This has actually been observed as indicated in Figs. 4 and 5 where the H- and E-plane patterns before and after optimization are provided for the selected frequencies.

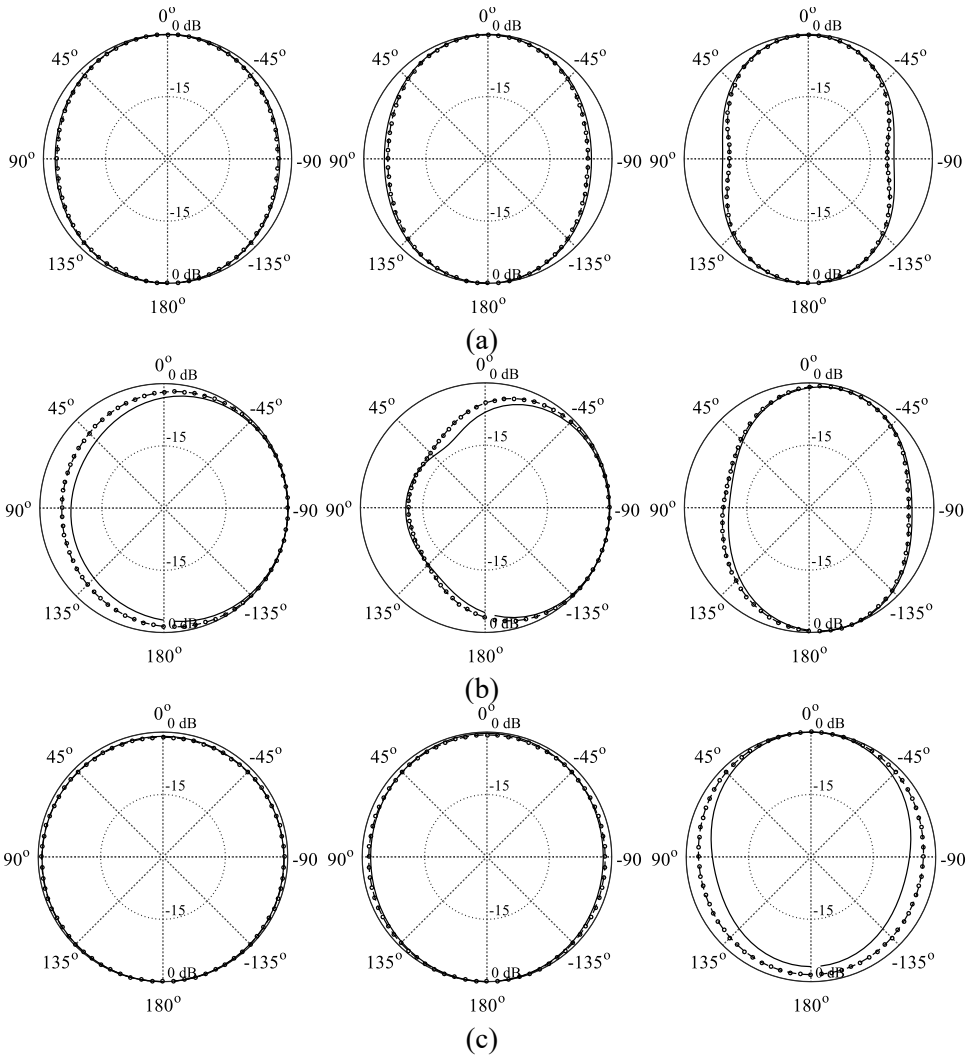

Fig. 4. H-plane radiation patterns before (—) and after (-o-) optimization for 4 GHz, 6 GHz, and 8 GHz: (a) Antenna I, (b) Antenna II, (c) Antenna III.

Table I also provides benchmarking against the previously reported procedures: Algorithm 2 (involving a smart gradient update scheme based on relative changes of the parameter values during optimization process; Koziel and Pietrenko-Dabrowska, 2019a), and Algorithm 3 (utilizing a sparse gradient update scheme with a Broyden formula applied for selected parameters; Koziel and Pietrenko-Dabrowska, 2019b; Pietrenko-Dabrowska, Koziel, 2019; for the details see Appendix). The procedure introduced in this paper outperforms both methods with respect to all the quality measures considered: the design quality and its standard

deviation, as well as the results stability. Algorithms 2 and 3 deliver lower computational savings of around 30 percent, and the design quality is considerably worse: objective function deterioration exceeds 1 dB w.r.t. the reference algorithm. In addition, the results repeatability is also inferior, especially for Algorithm 3 it is approximately twice as high as for the reference and the proposed algorithm.

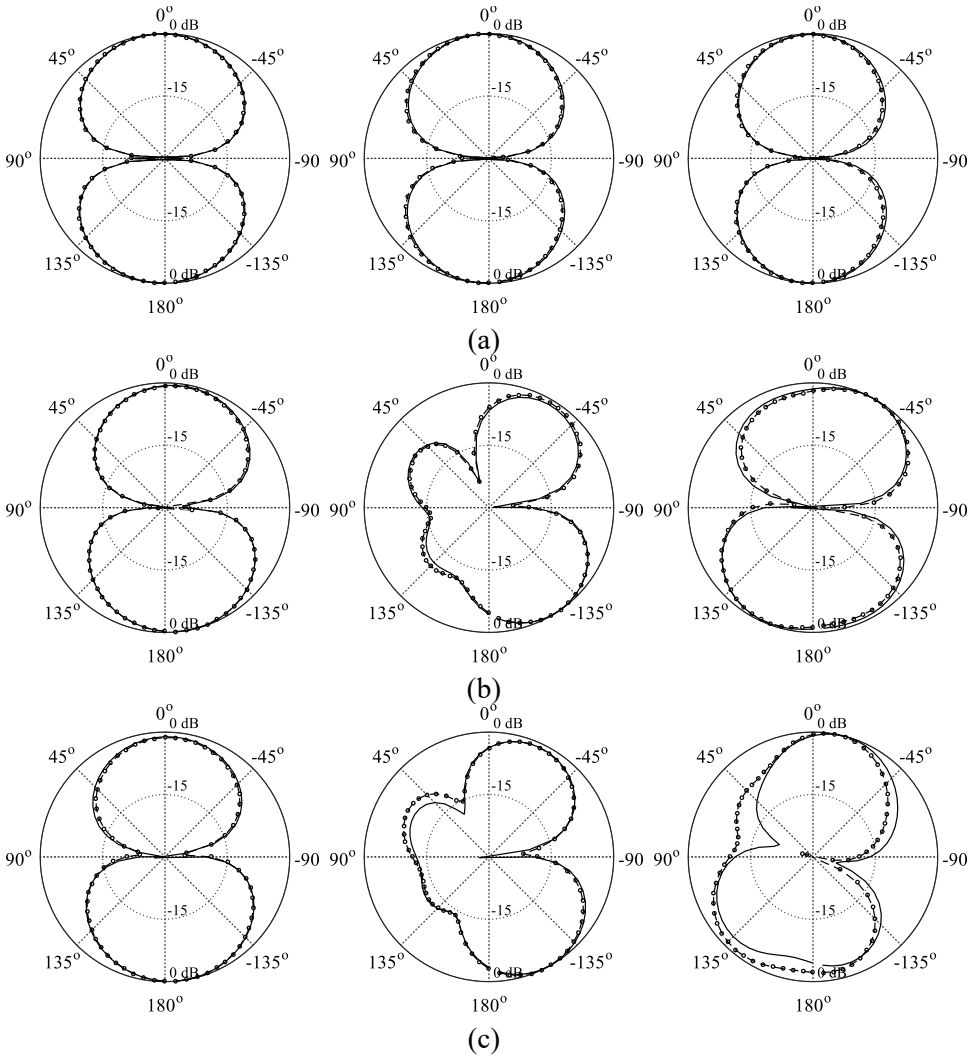

Fig. 5. E-plane radiation patterns before (—) and after (-o-) optimization for 4 GHz, 6 GHz, and 8 GHz: (a) Antenna I, (b) Antenna II, (c) Antenna III.

4. Conclusion

The paper presented a novel algorithm for expedited (local) design optimization of antenna structures. Our approach is based on the trust-region gradient search with numerical derivatives. It offers an improvement of computational efficiency by monitoring gradient alterations along the optimization path and by suppressing utilization of finite-differentiation-based updates whenever small sensitivity variations are detected. Verification studies demonstrate that the proposed approach outperforms recently reported accelerated TR procedures in terms of computational savings, along with the result reliability and design quality. The primary limitation of the approach is that—just as the reference TR algorithm—it is a local method, and a reasonably good initial design is required to ensure satisfactory outcome. Also, depending on the functional landscape of the considered objective function, the achieved computational savings may be lower than those presented in this work, although given the comprehensiveness of the verification process it is not very likely in practice. Potential uses of the proposed framework include direct EM-driven design closure as well as solving sub-problems for variable-fidelity surrogate-assisted routines (surrogate model extraction and optimization). Furthermore, the presented algorithm may be combined with the previously reported techniques (i.e., FD replacement with the Broyden formula for directions suitably aligned with the most recent design relocation and/or omission of FD depending on relative design relocation with respect to the current search region), which may potentially lead to additional computational saving and design quality improvement. This will be the subject of the future work.

Appendix: Gradient Search with Selective Broyden Updates

Here, the particulars of the algorithm with selective Broyden updates are briefly outlined, for a more detailed description see Koziel and Pietrenko-Dabrowska, 2019b. In the procedure, the initial estimate of the antenna response gradient is obtained through full finite differentiation. In subsequent iterations, FD is superseded for some variables with a rank-one Broyden formula (Koziel *et al*., 2010)

$$\boldsymbol{G}_S^{(i+1)}(f) = \boldsymbol{G}_S^{(i)}(f) + \frac{\left(\left(S_{11}\left(\boldsymbol{x}^{(i+1)}, f\right) - S_{11}\left(\boldsymbol{x}^{(i)}, f\right)\right) - \boldsymbol{G}_S^{(i)T}(f)\cdot \boldsymbol{h}^{(i+1)}\right)\cdot \boldsymbol{h}^{(i+1)}}{\boldsymbol{h}^{(i+1)T}\boldsymbol{h}^{(i+1)}},\ i = 0, 1, \quad (8)$$

where $\boldsymbol{G}_S^{(i)}(f)$ is the reflection gradient $\boldsymbol{G}_S(f) = [G_1(f)\ \ldots\ G_n(f)]^T = [\partial S_{11}(\boldsymbol{x},f)/\partial x_1\ \ldots\ \partial S_{11}(\boldsymbol{x},f)/\partial x_n]^T$ at the frequency f in the i-th iteration; and $\boldsymbol{h}^{(i+1)} = \boldsymbol{x}^{(i+1)} - \boldsymbol{x}^{(i)}$ denotes the recent design relocation. The choice of the gradient components to be updated by (8) is based on the alignment between $\boldsymbol{h}^{(i+1)}$ and the coordinate system vectors $\boldsymbol{e}^{(k)} = [0\ \ldots\ 0\ 1\ 0\ \ldots\ 0]^T$ (1 on the k-th position), $k = 1, \ldots, n$. This is quantified in the ith iteration as $\varphi_k^{(i+1)} = |\boldsymbol{h}^{(i+1)T}\boldsymbol{e}^{(k)}|/\|\boldsymbol{h}^{(i+1)}\|$ and compared to the alignment threshold φ_{min}, a control parameter of the algorithm. $G_k(f)$ is either estimated through FD (if $\varphi_k^{(i+1)} < \varphi_{min}$) or calculated using (8) (if $\varphi_k^{(i+1)} \geq \varphi_{min}$). Increasing the threshold φ_{min} makes a condition for using the Broyden formula more rigorous. On the other hand, lowering φ_{min} is advantageous from the computational savings point of view, however it may lead to design quality degradation.

Acknowledgement

The authors thank Dassault Systemes, France, for making CST Microwave Studio available. This work is partially supported by the Icelandic Centre for Research (RANNIS) Grant 174114051, and by National Science Centre of Poland Grant 2015/17/B/ST6/01857.

References

Alsath M.G.N. and Kanagasabai, M. (2015) "Compact UWB monopole antenna for automotive communications," *IEEE Trans. Ant. Prop.*, Vol. 63, No. 9, pp. 4204-4208.

Baratta, I.A., de Andrade, C.B., de Assis, R.R. and Silva, E.J. (2018) "Infinitesimal dipole model using space mapping optimization for antenna placement," *IEEE Ant. Wireless Prop. Lett.*, Vol. 17, pp. 17-20.

Bencivenni, C., Ivashina, M.V., Maaskant, R. and Wettergren, J. (2016) "Synthesis of maximally sparse arrays using compressive sensing and full-wave analysis for global earth coverage applications," *IEEE Trans. Ant. Prop.*, Vol. 64, No. 11, pp. 4872-487.

Cai, J., King, J., Yu, C., Liu, J. and Sun, L. (2018) "Support vector regression-based behavioral modeling technique for RF power transistors." *IEEE Microw. Wireless Comp. Lett.*, Vol. 28, No. 5, pp. 428-430.

Chavez-Hurtado, J.L. and Rayas-Sanchez, J.E. (2016) "Polynomial-based surrogate modeling of RF and microwave circuits in frequency domain exploiting the multinomial theorem." *IEEE Trans. Microwave Theory Techn.*, Vol. 64, No. 12, pp. 4371-4381.

Choi, K., Jang, D.H., Kang, S.I., Lee, J.H., Chung, T.K. and Kim, H.S. (2016) "Hybrid algorithm combining genetic algorithm with evolution strategy for antenna design," *IEEE Trans. Magn.*, Vol. 52, No. 3.

Conn, A.R., Gould, N.I.M. and Toint, P.L. (2000) *Trust Region Methods*, MPS-SIAM Series on Optimization.

Ghassemi, M., Bakr, M. and Sangary, N. (2013) "Antenna design exploiting adjoint sensitivity-based geometry evolution," *IET Microwaves Ant. Prop.*, Vol. 7, No. 4, pp. 268-276.

Goudos, S.K., Siakavara, K., Samaras, T., Vafiadis, E.E. and Sahalos, J.N. (2011) "Self-adaptive differential evolution applied to real-valued antenna and microwave design problems," *IEEE Trans. Antennas Propag.*, Vol. 59, No. 4, pp. 1286–1298.

Haq, M.A., Koziel, S. and Cheng, Q.S. (2017) "EM-driven size reduction of UWB antennas with ground plane modifications," *Int. Applied Comp. Electromag. Society (ACES China) Symposium*, China

Jacobs, J.P. (2016) "Characterization by Gaussian processes of finite substrate size effects on gain patterns of microstrip antennas", *IET Micro. Ant. Prop.*, Vol. 10, No. 11, pp. 1189-1195.

Koziel, S. (2015) “Fast simulation-driven antenna design using response-feature surrogates,” *Int. J. RF & Microwave CAE*, Vol. 25, No. 5, pp. 394-402.

Koziel, S., Bandler, J.W., Cheng, Q.S. (2010), “Robust trust-region space-mapping algorithms for microwave design optimization”, *IEEE Trans. Micro. Theory Tech.*, Vol. 58, No. 8, pp. 2166-2174.

Koziel, S. and Bekasiewicz, A. (2016) *Multi-objective design of antennas using surrogate models*, World Scientific, London.

Koziel, S. and Bekasiewicz, A. (2018) “Sequential approximate optimization for statistical analysis and yield optimization of circularly polarized antennas,” *IET Microwaves Ant. Prop.*, Vol. 12, No. 13, pp. 2060-2064.

Koziel, S. and Ogurtsov, S. (2014) “Design optimization of antennas using electromagnetic simulations and adaptive response correction technique,” *IET Microwaves, Antennas Prop.*, Vol. 8, No. 3, pp. 180-185.

Koziel S. and Pietrenko-Dabrowska A. (2019a) “An efficient trust-region algorithm for wideband antenna optimization”, *European Ant. Propag. Conf. (EuCAP)*, Krakow, Poland, pp. 1-5.
Koziel S. and Pietrenko-Dabrowska A. (2019b) “Accelerated antenna optimization using gradient search with selective Broyden updates,” *IEEE Ant. Prop. Symp. (APS)*, 2019.

Koziel, S. and Unnsteinsson, S.D. (2018) “Expedited design closure of antennas by means of trust-region-based adaptive response scaling”, *IEEE Antennas Wireless Prop. Lett.*, Vol. 17, No. 6, pp. 1099-1103.

Lalbakhsh, A., Afzal, M.U., Esselle, K.P. and Zeb, B.A. (2015) “Multi-objective particle swarm optimization for the realization of a low profile bandpass frequency selective surface,” *Int. Symp. Ant. Propag. (ISAP)*, Hobart, TAS, pp. 1-4.

Lalbakhsh, A., Afzal, M.U., Esselle, K.P. and Smith, S.L. (2017) “Design of an artificial magnetic conductor surface using an evolutionary algorithm,” *Int. Conf. Electromagn. Advanced Applications (ICEAA)*, Verona, Italy, pp. 885-887.

Lalbakhsh, A., Afzal, M.U. and Esselle, K.P. (2017) “Multiobjective particle swarm optimization to design a time-delay equalizer metasurface for an electromagnetic band-gap resonator antenna,” *IEEE Ant. Wireless Propag. Lett.*, Vol. 16, pp. 912-915, 2017.

Lalbakhsh, A., Afzal, M.U., Esselle, K.P. and Smith, S.L. (2019) “Wideband near-field correction of a Fabry–Perot resonator antenna,” *IEEE Trans. Ant. Propag.*, Vol. 67, No. 3, pp. 1975-1980.

Liu, B., Koziel, S. and Zhang, Q. (2016) “A multi-fidelity surrogate-model-assisted evolutionary algorithm for computationally expensive optimization problems,” *J. Comp. Science*, Vol. 12, pp. 28-37.

Nocedal, J. and Wright, S. (2006) *Numerical Optimization*. 2nd ed., Springer, New York.

Qing X. and Chen, Z.N. (2009) "Compact coplanar waveguide-fed ultra-wideband monopole-like slot antenna," *IET Microwaves Ant. Prop.*, Vol. 3, No. 5, pp. 889-898.

Pietrenko-Dabrowska, A and Koziel, S. (2019) "Numerically efficient algorithm for compact microwave device optimization with flexible sensitivity updating scheme," *Int. J. RF Microw. Comput. Aided Eng.*, Vol. 29:e21714, pp. 1-7.

Prado, D.R., López-Fernández, J.A., Arrebola, M. and Goussetis, G. "Support vector regression to accelerate design and crosspolar optimization of shaped-beam reflectarray antennas for space applications," *IEEE Trans. Antennas Propag.*, Vol. 67, No. 3, pp. 1659-1668.

Reyna, A., Balderas, L.I. and Panduro, M.A. (2017) "Time-modulated antenna arrays for circularly-polarized shaped beam patterns," *IEEE Ant. Wireless Prop. Lett.*, Vol. 16, pp. 1537-1540.

Richard, V., Loison, R., Gillard, R., Legay, H., Romier, M., Martinaud, J.-P., Bresciani, D. and Delepaux, F. (2019) "Spherical mapping of the second-order phoenix cell for unbounded direct reflectarray copolar optimization," *Progr. Electromagn. Res. C*, Vol. 90, pp. 109-124.

Saini, R.K. and Dwari, S. (2016) "A broadband dual circularly polarized square slot antenna," *IEEE Trans. Ant. Prop.*, Vol. 64, No. 1, pp. 290-294.

Siragusa, R., Perret, E., Lemaitre-Auger, P., Van Nguyen, H., Tedjini, S. and Caloz, C. (2012) "A tapered CRLH interdigital/stub leaky-wave antenna with minimized sidelobe levels", *IEEE Antennas Wireless Propag. Lett.*, Vol. 11, pp. 1214-1217.

Su, Y., Lin, J., Fan, Z. and Chen, R. (2017) "Shaping optimization of double reflector antenna based on manifold mapping," *Int. Applied Comput. Electromag. Society Symp. (ACES)*, pp. 1-2.

Ullah, U. and Koziel, S. (2018) A broadband circularly polarized wide-slot antenna with a miniaturized footprint," *IEEE Ant. Wireless Prop. Lett.*, Vol. 17, No. 12, pp. 2454-2458.

Vendik, I.B., Rusakov, A., Kanjanasit, K., Hong, J. and Filonov, D. (2017) "Ultrawideband (UWB) planar antenna with single-, dual- and triple-band notched characteristic based on electric ring resonator," *IEEE Ant. Wireless Prop. Lett.*, Vol. 16, pp. 1597-1600.

de Villiers, D.I.L., Couckuyt, I. and Dhaene, T. (2017) "Multi-objective optimization of reflector antennas using kriging and probability of improvement," *Int. Symp. Ant. Prop.*, pp. 985-986, San Diego, USA.

Wang, J., Yang, X.S. and Wang, B.Z. (2018) “Efficient gradient-based optimization of pixel antenna with large-scale connections,” *IET Microwaves Ant. Prop.*, Vol. 12, No. 3, pp. 385-389.

Zaharis, Z.D., Gravas, I.P., Yioultsis, T.V., Lazaridis, P.I., Glover, I.A., Skeberis, C. and Xenos, T.D. (2017) “Exponential log-periodic antenna design using improved particle swarm optimization with velocity mutation,” *IEEE Trans. Magn.*, Vol. 53, No. 6.

Zhou, M., Borries, O. and Jørgensen, E. (2015) “Design and optimization of a single-layer planar transmit-receive contoured beam reflectarray with enhanced performance,” *IEEE Trans. Antennas Propag.*, Vol. 63, No. 4, pp. 1247-1254.